10th International Conference on Composite Science and Technology
ICCST/10
(Editors)

THE IDENTIFICATION OF ELASTIC PROPERTIES OF COMPOSITE MATERIALS BY MODAL ANALYSIS APPROACH

Nan LI, Mabrouk BEN TAHAR, Zoheir ABOURA, Kamel KHELLIL

Sorbonne universités, Université de technologie de Compiègne
Laboratoire Roberval, UMR 7337 UTC-CNRS
{*nan.li, mabrouk.bentahar, zoheir.aboura, kamel.khellil*}*@utc.fr*

Keywords: Composite materials, Stitched composite, Modal analysis, FEM plate element

Summary: *The identification of elastic properties of composite material is of great significance for various industrial fields such as automotive, train industry and aerospace. The static mechanical tests show their limitations in the identification of composite materials with complex reinforcement due to the complexity of representative volume element and the effect of scale. An identification method based on the correlation of measured and calculated dynamic behavior is proposed to overcome these limitations. A mode classification process is conducted to accelerate the identification. Every constant is identified by minimizing the difference between the calculated and the measured frequencies of the group that it dominates. This method has been applied to two types of composite plate: unstitched plate and stitched plate.*

1. Introduction

The variety of constituents and moulding technique of composite materials leads to a great diversity of their properties. On the one hand, this characteristic brings us a certain degree of freedom in the optimization of their performance according to different areas of applications and desired functionality; on the other hand, it requires an identification for each configuration of fabrication.

The mechanical test is a traditional way to identify the elastic properties. For composite materials which are heterogeneous, the specimen is sometimes not big enough to achieve a satisfied level of homogenization. In addition, the exact values of some properties are difficult to obtain by classical mechanical test such as the in-plane shear modulus of a thin plate.

To overcome the difficulties in the identification of elastic properties of composite materials, an alternative method of identification from the vibration behavior has been proposed in the last two decades. The vibration behavior of a structure is controlled by the elastic properties. Inversely, the elastic properties can be determined by the vibration behavior via a sufficiently accurate model. Based on this principle, the identification is realized by minimizing the difference between the measured result of vibration behavior and the result calculated by a model. More details about the evolution of this method can be found in [1].

In this paper, we propose an identification method from experimental vibration result through mode classification. Our method presents several advantages:

• In terms of numerical model, an efficient finite element model with high accuracy and relatively short calculation time is introduced. The former merit guarantees a lower level of model error and the latter accelerates the identification process.

• In terms of experiment, a combination of shaker and vibrometer is chosen. The shaker can offer a larger band of excitation in time compared to a hammer and in space compared to a loudspeaker. As a result, the shaker is a proper companion for vibrometer. The mechanical test is also carried out and the difficulty is fully discussed. The results of the mechanical test are used as the initial values of the finite element model.

• The identification is based on mode classification which enables the identification of one parameter with minimum influence of the others. The coupled modes will be used to verify the whole identification. More than 20 modes are used in the whole process.

• This approach is proved to be effective on the composite plate and stitched plate (To our knowledge, this is the first time that this method has been applied to stitched plate).

2. Finite element model

For a thin plate, the Kirchhoff hypothesis is widely used in the literatures. In the continuous Kirchhoff theory, the transverse shear strain is imposed to be zero on the whole domain. This assumption requires C^1 continuity for β_x and β_y. The discrete Kirchhoff theory relaxes a little this strict assumption and imposes the transverse shear strain to be zero only on some discrete points of the boundary of an element. The discrete Kirchhoff elements started from DKT[2] and DKQ[3] and have formed a big family [4]. Based on the DKQ element, a discrete Kirchhoff quadrilateral element with in-plane displacement is proposed (Figure 1).

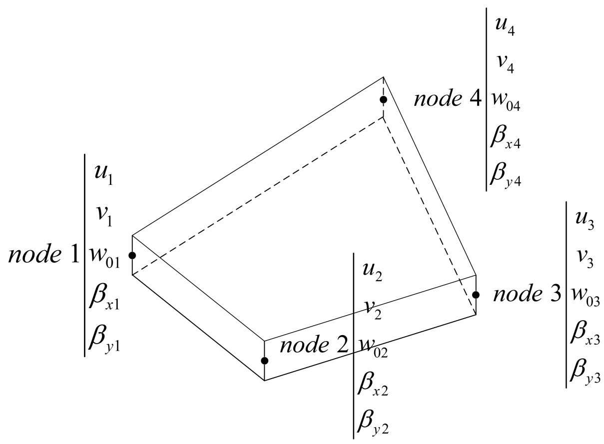

Figure 1. Quadrilateral element with in-plane DOF

The explicit expression of shape functions of β_x and β_y can be found in [3]. As for transverse displacement w_0, no interpolation function is needed to develop the stiffness matrix. However, the interpolation function is necessary to develop the mass matrix. w_0 is expressed quadratically over the element in our work. The explicit expression of w_0 can be found in [5].

The in-plane displacement can be expressed independently in terms of the nodal in-plane DOF through a linear interpolation of Q4 element.

The stiffness matrix can be derived from the strain energy:

$$\begin{aligned} U &= \frac{1}{2}\int_{\Omega} \langle\varepsilon\rangle \{\sigma\}\, d\Omega \\ &= \frac{1}{2}\int_{A} \langle q^e\rangle [B]^T [T]^T \int_{-\frac{t}{2}}^{\frac{t}{2}} [F(z)]^T [C] [F(z)]\, dz\, [T]\, [B] \det J d\xi d\eta \{q^e\}, \end{aligned} \tag{1}$$

where

$$[F(z)] = \begin{bmatrix} 1 & 0 & 0 & 0 & z & 0 & 0 & 0 \\ 0 & 0 & 0 & 1 & 0 & 0 & 0 & z \\ 0 & 1 & 1 & 0 & 0 & z & z & 0 \end{bmatrix}, [T] = \begin{bmatrix} j & 0_{2\times2} & 0_{2\times2} & 0_{2\times2} \\ 0_{2\times2} & j & 0_{2\times2} & 0_{2\times2} \\ 0_{2\times2} & 0_{2\times2} & j & 0_{2\times2} \\ 0_{2\times2} & 0_{2\times2} & 0_{2\times2} & j \end{bmatrix},$$

$$[C] = \begin{bmatrix} E_1/(1-E_2\nu_{12}^2/E_1) & \nu_{12}E_2/(1-E_2\nu_{12}^2/E_1) & 0 \\ \nu_{12}E_2/(1-E_2\nu_{12}^2/E_1) & E_2/(1-E_2\nu_{12}^2/E_1) & 0 \\ 0 & 0 & G_{12} \end{bmatrix}.$$

$[C]$ is the stress-strain relation matrix of an orthotropic plate under plane stress (the x-y-z coordinate system is the same as the material orthotropic coordinate system).

The mass matrix is derived from the kinetic energy:

$$\begin{aligned} K &= \frac{1}{2}\omega^2\rho\int_{\Omega} \langle u\rangle \{u\}\, d\Omega \\ &= \frac{1}{2}\omega^2\rho \langle q^e\rangle \int_{A} [B_u]^T \int_{-\frac{t}{2}}^{\frac{t}{2}} [F_u(z)]^T [F_u(z)]\, dz\, [B_u] \det J d\xi d\eta \{q^e\}. \end{aligned} \tag{2}$$

3. Experiments

3.1 Fabrication

We fabricated two plates: one is unstitched composite plate and the other is stitched composite plate. Both plates are made of 10 plies of woven 5 harness satin carbon fiber fabric and epoxy resin and molded by Vacuum Assisted Resin Infusion Molding technique. After molding, the plates were kept at 80°C for 24 hours. For the stitched plate, a technique called one-side stitching (Figure 2) was employed to stitch the dry fabrics by a robot KUKA. This technique uses two needles and a single thread. One needle which inclines 45°wears the thread and penetrates the dry fabrics; the other needle which is actually a hook will pick up the thread and takes it to another side. Each stitch is 25mm in width. Instead of being completely covered by the stitches, the stitched plate was stitched dispersedly in order to concentrate on the property of the stitch itself and avoid involving the property between stitches. Detailed distribution of the stitches and the dimension of the plate are show in Figure 3(b).

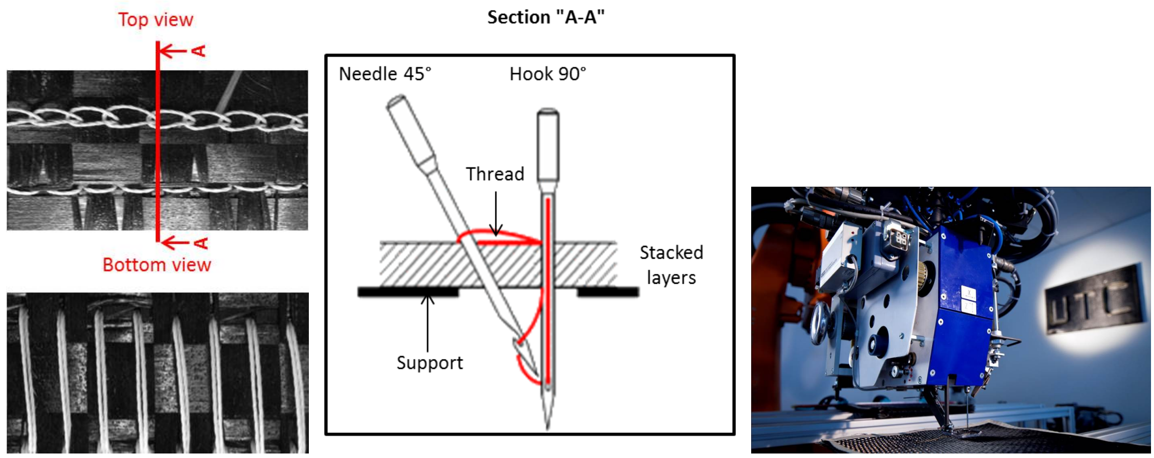

(a) Top/Bottom view of stitch

(b) Section A-A

(c) Robot KUKA

Figure 2. One Side Stitching

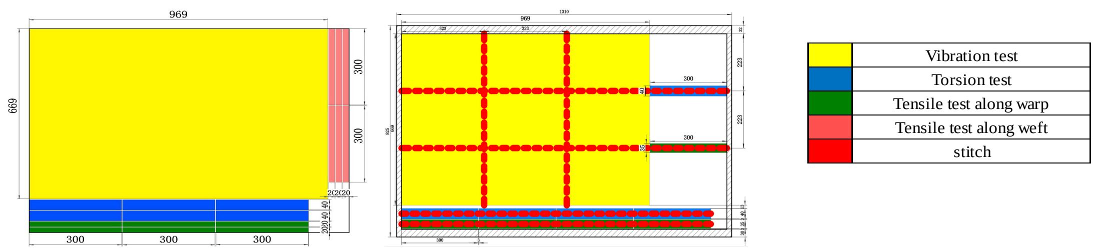

(a) unstitched plate

(b) stitched plate

Figure 3. The test specimen for different tests

3.2 Mechanical test

3.2.1 Tensile test

A traditional tensile test with bidirectional gauge was conducted on the specimen of both unstitched plate and stitched plate. The number and dimension of specimen are shown in Figure 3.

3.2.2 Torsion of a rectangle section bar

For orthotropic materials, a torque will generate two shear stress τ_{12} et τ_{13} on the section perpendicular to the torque axis. Therefore, two shear moduli will be involved in the torsion test. According to the theory of anisotropic elastic body developed by Lekhnitskii [6] in 1963, the relationship between these two shear moduli is as follows:

$$G_{ij} = \left[\frac{C}{\theta}\right] \frac{L}{ba^3\beta\,(m)} \qquad (i, j = 1, 2, 3)\,, \tag{3}$$

where

$$\beta(m) = \frac{32m^2}{\pi^4} \sum_{i=1,3,5...}^{n} \frac{1}{i^4} \left(1 - \frac{2m}{i\pi} \mathrm{th} \frac{i\pi}{2m}\right) \tag{4}$$

and

$$m = \frac{b}{a}\sqrt{\frac{G_{ik}}{G_{ij}}} \qquad k \neq i, j. \tag{5}$$

θ is the angle of twist; C is the applied torque ; b is the width of the sample; a is the thickness of the sample; L is the distance between the two jaws.

If we choose the specimen of rectangle section, we can favor a shear modulus over the other by controlling the geometry of the specimen. According to equation 4, when m is bigger than 5, β converges to a certain value. This condition can be easily fulfilled by choosing the ratio b/a bigger than 7 as G_{ik}/G_{ij} varies from 0.5 to 1.5 according to [7]. Then the shear modulus can be obtained by equation 3. In our test, the ratio b/a of all the specimen is bigger than 8 and the module obtained is shown in Table 1.

3.3 Vibration test

The setup for the vibration test is illustrated in Figure 4. The test plate is suspended with two thin strings and excited by white noise signal through a shaker (Brüel & Kjær). The vibration velocity amplitude is captured by a 1D laser vibrometer (Polytec).

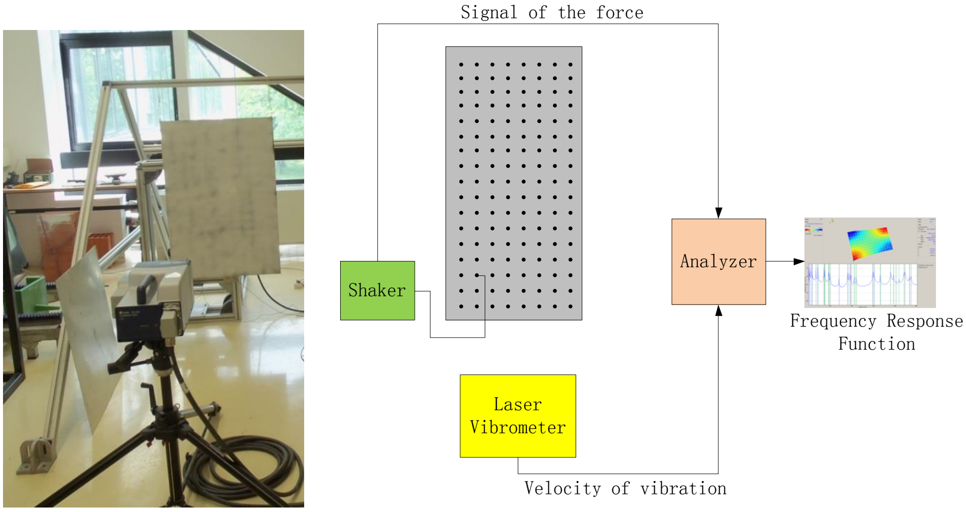

Figure 4. The setup of the vibration test

4. Methodology

The result of the mechanical tests is used as the initial values of the finite element model which exports the calculated frequencies and mode shapes. Meanwhile, measured resonance frequencies and mode shapes are obtained by vibration test. By observing both the measured and calculated modes shapes, the modes can be divided into several groups. Each group has its dominating parameter, which can be verified by sensitivity analysis of parameters. Within one group, the dominating parameter is updated in each iteration in order to minimize the difference between the calculated frequencies and the measured frequencies. At the same time, the Modal Assurance Criterion is calculated to guarantee the consistency of corresponding modes. An optimized result is obtained when the difference of frequencies is small enough. The whole identification process which is shown in Figure 5.

Among the four elastic constants of orthotropic plate under plane stress, the Poisson's ratio varies in a very narrow interval. Its influence on the natural frequencies can be neglected in most cases (except for some specials cases which have already been excluded [8]). In addition, we can see from Table 1 that the mechanical test already provides a satisfactory result of Poisson's ratio with acceptable standard deviation. So the Poisson's ratio is fixed as the mechanical value in this work. The identification process will focus on the other three elastic constants.

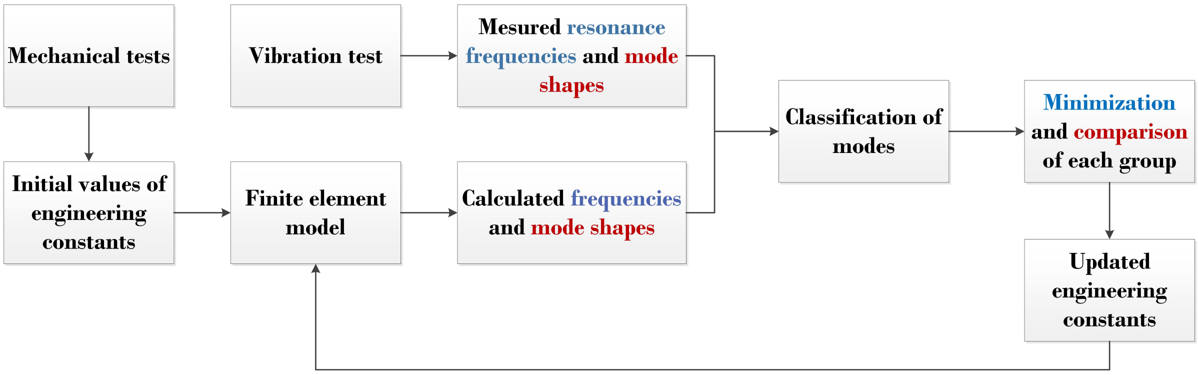

Figure 5. The flowchart of the identification

5. Application

5.1 First application—the unstitched plate

5.1.1 Result of mechanical test and vibration test

The 4 constants of in-plane properties obtained by mechanical test are listed in Table 1. The result of vibration test is listed in Table 3 (f_{Mea}).

E_1(warp)[Gpa]	E_2(weft)[Gpa]	ν	G_{12}[Gpa]
$47.872^{\pm 4.8}$	$45.143^{\pm 2.6}$	$0.11^{\pm 0.028}$	$5.818^{\pm 0.36}$

Table 1. The properties obtained by mechanical test

5.1.2 Identification based on correlation experiment-calculation

The identification is divided into three steps: (1) Categorization of modes according to different behaviors; (2) Determination of the parameter which dominates a group; (3) Identification of the dominating parameter of corresponding group.

Through observation of modes shapes coming from vibration test, the modes can be divided into the following groups: (a) torsional modes; (b) bending modes along direction X; (c) bending modes along direction Y; (d) mixed modes. The representative of each family is presented in Figure 6.

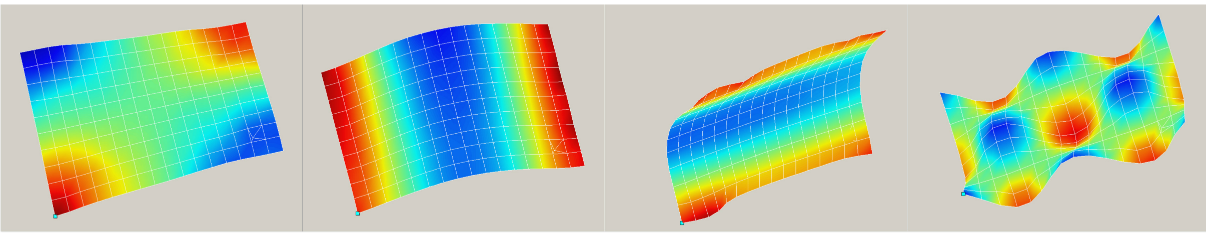

Figure 6. (a) a torsional mode (b) a bending mode along direction X (c) a bending mode along direction Y (d) a mixed mode

The classification of modes is followed by determination of the parameter which dominates a group. We take the bending mode along direction X as an example. In this case, the plate can be treated as a beam. According to the analytical solution of beam, this group is dominated by E_1. An analysis of sensitivity of the parameters in the finite element model can also confirm this statement (Table 2). Two groups of parameters with the same E_1 but different E_2 and G_{12} are injected into the finite element model but the gap caused by this difference is small enough to be neglected. So the bending group along direction X is dominated by E_1. The same process can be applied to the other groups (a,b,c). So the bending group along direction Y is dominated by E_2; the torsional group is controlled by G_{12}. The mixed group is more complicated and controlled by all the parameters.

Number of mode	**E_1=47.872 E_2=45.143 G_{12}=5.818**	**E_1=47.872 E_2=40 G_{12}=3**	**Gap%**
2	33.66	33.65	-0.04
6	92.58	92.39	-0.20
10	180.39	180.22	-0.10
16	297.67	297.34	-0.11

Table 2. Analysis of sensibility of parameters in element finite model (group b)

Then, the parameters are identified by minimizing the gap between the experimental frequencies and the calculated frequencies of the group they dominate. The mixed modes are not involved in the identification of each parameter but act as a global validation in the end. They are used to confirm the result and the whole identification process.

5.1.3 Result and discussion

The result of the mechanical test is used as the initial values of finite element model. The natural frequencies using these initial values are listed in Table 3 (f^1_{Cal}). The errors of several modes are significant. With the method introduced in Section 5.1.2, the differences between the calculated frequencies and the measured frequencies diminish to an acceptable level (Table 3). We can see that the average difference of all the 23 modes is only 1.14%. The identified constants are listed in Table 4. The difference of the Young's modulus is about 5%. In fact, due to the heterogeneous property of the material and the relative small size of the gauge, the result of mechanical test also has a dispersion of the same level. So this difference is reasonable.

As to the shear modulus, however, the difference is significant. In fact, this result is predictable because the measurement of shear moduli by mechanical test is always delicate. N.Tableau [9] has proved that the measurement of twist angle near the two jaws is biased by the load introduction and cannot reflect the intrinsic characteristics of the tested material. The measurement of the twist angle should be in restrained zone at the center of the specimen. Stereo correlation can be a solution in this case but burdensome instruments and complex process should be tolerated. In addition, we should notice that although a shear modulus is favored over the others there is still the influence of the other (G13).

The method we used in the mechanical test is deliberately simplified and easy to conduct. It gives us an idea of the initial values to start the identification process (although it is away from the real value).

5.2 Second application —the stitched plate

5.2.1 Result of the mechanical test and vibration test

The constants of in-plane properties obtained by mechanical test are listed in Table 5. The result of vibration test is listed in Table 6 (f_{Mea}).

5.2.2 Identification based on correlation experiment-calculation

The stitched plate contains three domains (Figure 7): the unstitched part (III), the stitches along the direction X (II) and the stitches along the direction Y (I). Compared to other parts, the intersections of the stitches along two directions are very small and are considered to have the same properties as the stitch along X.

As to the unstitched part, because a thin layer of resin was added on the surface after moulding to improve the surface flatness, the property of the unstitched zone is considered as the homogenization of the thin resin and the optimized result of the unstitched plate. After a simple calculation, the property of the unstitched zone is fixed to 80% of the optimized result of the unstitched plate. The property of the unstitched domain is kept unchanged during the identification process of the stitched plate. In regard to the stitch along X, E^{II}_x and G^{II}_{xy} are provided by the mechanical test; while E^{II}_y which cannot be obtained by mechanical test is given an initial value of 39.5Gpa. As no mechanical tests are conducted on stitch along Y, the initial values can

$N°$	f_{Mea}	f^1_{Cal}	Error %	f^2_{Cal}	Error %	Group
1	15,3125	19,0458	24,38	15,2757	-0,24	Torsion
2	34,6875	33,6622	-2,96	34,2127	-1,37	Bending X
3	43,7500	49,4597	13,05	44,0504	0,69	Mixed
4	70,9375	68,2657	-3,77	69,9978	-1,32	Bending Y
5	75,0000	76,4887	1,98	74,6617	-0,45	Mixed
6	92,8125	92,5766	-0,25	93,9830	1,26	Bending X
7	94,0625	105,1095	11,74	95,7767	1,82	Mixed
8	100,3125	106,2761	5,94	101,8474	1,53	Mixed
9	140,6250	158,3410	12,60	144,0481	2,43	Mixed
10	180,3125	180,3912	0,04	183,3513	1,69	Bending X
11	186,5625	193,8029	3,88	188,0524	0,80	Mixed
12	193,4375	186,2330	-3,72	194,1083	0,35	Bending Y
13	195,9375	194,6142	-0,68	196,2436	0,16	Mixed
14	210,9375	219,5092	4,06	213,0786	1,02	Mixed
15	220,0000	240,8351	9,47	225,7899	2,63	Mixed
		265,1538*		248,8336*		
16	296,5625	297,6726	0,37	302,5403	2,02	Bending X
17	302,5000	310,3628	2,60	309,9337	2,46	Mixed
		339,6573*		315,8702*		
18	330,9375	353,0453	6,68	339,8644	2,70	Mixed
		366,5048*		375,8196*		
19	378,4375	373,7376	-1,24	379,9624	0,40	Mixed
20	391,8750	394,3347	0,63	393,1522	0,33	Mixed
21	404,0625	444,4516	10,00	417,2004	3,25	Mixed
22	417,5000	435,5409	4,32	423,1458	1,35	Mixed
23	439,6875			451,4924	2,68	Bending Y
		Max error	24,38	**Max error**	3,25	
		Min error	-3,77	**Min error**	-1,37	
		Average error	4,51	**Average error**	1,14	

[*] These modes are not found in experiment.
[1] Whose input is the result of mechanical test.
[2] Whose input is the identified parameters

Table 3. The obtained frequency match using mechanical values and the identified values

	E_1[Gpa]	E_2[Gpa]	G_{12}[Gpa]
Identified value	49.5	47.5	3.2
Mechanical test	47.872	45.143	5.818
Difference%	3.4	5.22	-45

Table 4. The identified value of the elastic constants and the comparison with the result of the mechanical test

E_1(warp)[Gpa]	E_2(weft)[Gpa]	ν	G_{12}[Gpa]
$38.901^{\pm 1.3}$	–	$0.04^{\pm 0.002}$	$5.197^{\pm 0.42}$

Table 5. The properties obtained by mechanical test

only be obtained through some assumptions. Given that the ratio of anisotropy of the unstitched plate is α ($\frac{E_x^{III}}{E_y^{III}} = \alpha$), we can assume the ratio of E_x^{II} and E_y^{I} is also α because their difference is due to the anisotropy of the basic fabric. The moduli of the other direction E_x^{I} and E_y^{II} conform to the same relation. The above assumptions lead to

$$\frac{E_x^{II}}{E_y^{I}} = \alpha, \frac{E_x^{I}}{E_y^{II}} = \alpha. \tag{6}$$

Based on equation 6, one relation between the four moduli can be established. The shear moduli of the stitches along the two directions are assumed to be equal:

$$G_{xy}^{I} = G_{xy}^{II}. \tag{7}$$

Equation 6 and 7 are not only used to obtain the initial values of some constants which are not available in mechanical test, but also respected during the identification process. The other parts of the identification are the same as the unstitched plate.

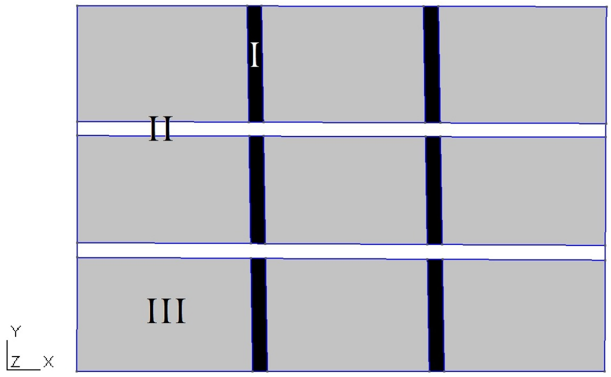

Figure 7. The partition of different domains

5.2.3 Result and discussion

The identification result of the stitched plate is summarized in Table 6, Table 7 and Figure 8. The differences of all the modes are within 5% and the average difference is only 0.16%. The identification quality is also guaranteed by some modes at high frequencies which have complex mode shapes and sensitive to the stitch. In Figure 8, the stitch can be seen in the mode shapes of vibration test. We can see that the stitches play an important role in the modes at high frequencies. The experiment-calculation differences of these modes are small. For example, the 25th mode at 409Hz is approximated by the finite element model with a difference of only 1.11%.

In Table 7,the fact that $E_y^{II} > E_x^{II}$ et $E_x^{I} > E_y^{I}$ can be explained by the geometry of the stitch. As shown in Figure 2(a), the stitch left one thread along the direction in width every step. These threads became rigid bars under the embracement of resin. Unlike the thread along direction in length which can only reinforce two edges of the stitch, these threads reinforce the whole surface.

$N°$	f_{Mea}	f_{Cal}	**Error** %	**Group**	$N°$	f_{Mer}	f_{Cal}	**Error** %	**Group**
1	15	15,41	2,73	Torsion	17	280*			Mixed
2	34	34,08	0,22	Bending X	18	300	299,04	-0,32	Bending X
3	43	43,98	2,27	Mixed	19	303*	304,96		Mixed
4	72	69,82	-3,03	Bending Y	20	322*	312,86		Mixed
5	77	74,41	-3,36	Mixed	21	336	336,03	0,01	Mixed
6	91	93,55	2,80	Bending X	22	379	368,39	-2,80	Bending Y
7	96	95,38	-0,64	Mixed	23	387	371,92	-3,90	Mixed
8	98	100,98	3,04	Mixed	24	398	386,72	-2,83	Mixed
9	141	142,70	1,21	Mixed	25	409	413,54	1,11	Mixed
10	176	180,34	2,47	Bending X	26	425	419,09	-1,39	Mixed
11	185	185,42	0,23	Mixed	27	428	449,03	4,91	Bending X
12	194	193,03	-0,50	Mixed	28	443	453,50	2,37	Mixed
13	199	195,35	-1,84	Mixed			**Max error**	4.91	
14	212	211,62	-0,18	Mixed			**Min error**	-3,90	
15	220	223,22	1,46	Mixed			**Average error**	0.16	
16	247	246,84	-0,06	Mixed					

* These modes shapes are not very clear.

Table 6. The obtained frequency match using the identified values

		E_x^{II}	E_y^{II}	G_{xy}^{II}
Stitch along X	Identified value	36.177	38.5	3
	Mechanical test	38.901	-	5.197
	Difference	-7%	-	-42%
		E_y^{I}	E_x^{I}	G_{xy}^{II}
Stitch along Y	Identified value	34.716	40.121	3
	Mechanical test	-	-	-
	Difference	-	-	-

Table 7. The identified value of the elastic constants and the comparison with the result of the mechanical test

6. Conclusion

An identification approach of elastic properties of composite plate from vibration test is presented in this work. This approach has been applied to two types of composite plate. For the unstitched plate, the identified Young's moduli along two directions are close to the result of the mechanical test. The measurement of the torsion modulus is difficult via mechanical test, while this method offers an alternative way to obtain it. In addition, to the authors' knowledge, this method has been applied to a stitched plate for the first time. This plate is heterogeneous not only on the scale of the stitch itself but also on the global scale of the positions of stitches on the plate. Although some hypotheses have been proposed to reduce the number of parameters to identify, this case can be a good start point of the application of this method to complex heterogeneous structure.

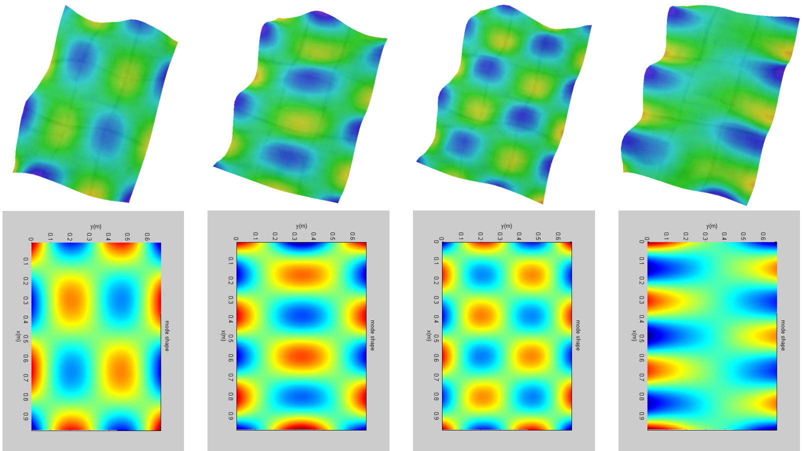

(a) 16^{th} mode (b) 21^{th} mode (c) 25^{th} mode (d) 28^{th} mode

Figure 8. The experimental (first raw) and corresponding calculated (second raw) mode shapes of several modes

Acknowledgments

The financial support from the China Scholarship Council is gratefully acknowledged.

References

[1] Shun-Fa Hwang, Jen-Chih Wu, and Rong-Song He. Identification of effective elastic constants of composite plates based on a hybrid genetic algorithm. *Composite Structures*, 90(2):217–224, 2009.

[2] Jean-Louis Batoz, Klaus-JÜRgen Bathe, and Lee-Wing Ho. A study of three-node triangular plate bending elements. *International Journal for Numerical Methods in Engineering*, 15(12):1771–1812, 1980.

[3] Jean-Louis Batoz and Mabrouk Ben Tahar. Evaluation of a new quadrilateral thin plate bending element. *International Journal for Numerical Methods in Engineering*, 18(11):1655–1677, 1982.

[4] JL Batoz, CL Zheng, and F Hammadi. Formulation and evaluation of new triangular, quadrilateral, pentagonal and hexagonal discrete kirchhoff plate/shell elements. *International journal for numerical methods in engineering*, 52(5-6):615–630, 2001.

[5] Jean-Louis Batoz and Gouri Dhatt. Modelisation des structures par element finis, vol. 2. poutres et plaques. *Hermes, Paris*, 1990.

[6] S. G. Lekhnitskiĭ. *Theory of elasticity of an anisotropic elastic body*. Holden-Day, 1963.

[7] Julien Schneider, Zoheir Aboura, Kamel Khellil, Malik Benzeggagh, David Marsal, et al. Caractérisation du comportement hors-plan d'un tissé interlock= off-plan behaviour investigation of an interlock fabric. *Recueil des résumés et comptes rendus des 16èmes Journées Nationales sur les Composites*, 2009.

[8] Tom Lauwagie, Hugo Sol, Gert Roebben, Ward Heylen, Yinming Shi, and Omer Van der Biest. Mixed numerical–experimental identification of elastic properties of orthotropic metal plates. *Ndt & e international*, 36(7):487–495, 2003.

[9] Nicolas Tableau, Kamel Khellil, and Zoheir Aboura. Contribution to the accurate measurement of in plane and out of plane shear properties of composite materials. In *15th European Conference on Composite Materials*.